Molecular Crystals and Liquid Crystals Science and Technology. Section A. Molecular Crystals and Liquid Crystals

Publication details, including instructions for authors and subscription information:
http://www.tandfonline.com/loi/gmcl19

Positional and Charged Effects of Heterocyclic N Atoms on Mesogenic Properties of Stilbazoles and Analogous N-Oxides

Hong-Cheu Lin [a] , Long-Li Lai [a] , Yu-Sheng Lin [a] , Chiitang Tsai [b] & Rong-Chi Chen [b]

[a] Institute of Chemistry, Academia Sinica

[b] Institute of Applied Chemisty, Chinese Culture University, Taipei, Taiwan, Republic of China

Version of record first published: 24 Sep 2006

Mol. Cryst. Liq. Cryst., Vol. 339, pp. 55-71
Reprints available directly from the publisher
Photocopying permitted by license only

Positional and Charged Effects of Heterocyclic N Atoms on Mesogenic Properties of Stilbazoles and Analogous N-Oxides

HONG-CHEU LIN[a*], LONG-LI LAI[a*], YU-SHENG LIN[a], CHIITANG TSAI[b] and RONG-CHI CHEN[b]

[a]*Institute of Chemistry, Academia Sinica and* [b]*Institute of Applied Chemistry, Chinese Culture University, Taipei, Taiwan, Republic of China*

(Received May 28, 1997)

The synthesis and the phase behavior of stilbazoles and corresponding N-oxides containing different positions of heterocyclic N atoms, i.e. trans-2′-, 3′-, 4′- stilbazoles and their N-oxides, are reported. Their phase transition temperatures and the mesogenic behavior were investigated through the DSC, polarizing optical microscope and X-ray diffraction (XRD) measurements. Increasing dipole moments by oxidation of stilbazoles to analogous N-oxides induces the S_A phase with an interdigitated bilayer packing. Both 2′-stilbazoles and analogous N-oxides do not possess mesogenic phases, which may be due that π electron polarizabilities are reduced by the molecular twist originated from dipoles along the ortho-direction. Besides, the positonal effects of the N-oxides on mesogenic properties are more distinct than those of analogous stilbazoles, and new mesogenic phases have been generated by tuning the position of the N-oxide function in the charged liquid crystals. Consequently, unique mesogenic properties may be introduced through adjusting the dipolar direction and strength of the heterocyclic atoms in the molecules.

Keywords: positional effects; charged liquid crystals; stilbazoles; N-oxides; X-ray diffraction (XRD); interdigitated bilayers

INTRODUCTION

Liquid crystalline materials containing N-heterocyclic rings as the central rigid cores or as the terminal rigid cores are of current interest[1-4] due to several reasons. Compared with corresponding benzene analogues, the lone pair electrons of the nitrogen atom produce significant dipole moments which may enhance

* Authors for correspondence.

attractive forces to generate or to improve mesogenic properties.[5, 6] In case of the central rigid cores containing charged N-oxide functions, the N-oxide functions do really introduce attractive forces to stabilize S_A phase.[7] Whereas, in order to introduce lateral dipoles attaching lateral substituents[8–12] on the rigid cores are normally adopted in the structure design, which may cause the system broading and depress the mesogenic range. Nevertheless, dipole moments produed by the lone pair electrons of the N-heterocyclic rings can avoid the drawback of the system broading. Another benefit of the molecular design is that the direction and the strength of the dipole moment can be adjusted easily, such as changing the position of the N atom or oxidation of the N atom to the N-oxide function. By changing these factors the physical properties, such as response time, viscosity, dielectric constant, dipole moment, refractive index, mesogenic phase, phase transition temperature and molecular packing can be modified.

With regard to N-heterocyclic rings as the terminal rigid cores, the lone pair *electrons could* be suitable candidates as the proton acceptors for hydrogen-bonded supramolecules. There are several hydrogen-bonded supramolecules utilizing stilbazoles and stilbazole-N-oxides as the H-bond acceptors.[13] Therefore, the directional and charged effects of these dipoles can be both investigated in the pure systems along with the H-bonded systems. However, only a few charged liquid crystals with the N-oxides as the terminal rigid cores have been studied.[14, 15] So far, no systematic structural studies of stilbazoles and their N-oxides with different N atom positions have been described. To our knowledge, the only stilbazole-N-oxide as the H-bond acceptor was trans-4-hexyloxy-4′-stilbazole-N-oxide up to date and it does not possess any mesogenic properties as described.[16] Herein, we wish to report the synthesis and characterization of new series of mesogenic trans-stilbazoles and their N-oxides in comparison with trans-4-alkoxy-4′-stilbazoles which have been reported previously.[17] Furthermore, the positional and dipolar effects of the N atoms as well as the N-oxides on mesogenic properties and molecular packings will be discussed. In this paper trans-stilbazoles are denoted as CnO, CnM and CnP, where n in Cn is the n-alkyloxy chain length OCnH2n+1 (n=8, 12 and 16) and the character (**O, M** and **P**) after n is the position of the N atom prepared from *o*-, *m*- and *p*- pyridinecarboxaldehyde **1**. Their corresponding N-oxides are abbreviated to CnOO, CnMO and CnPO, where the last character O means the N-oxide.

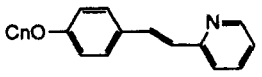

CnO

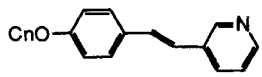

CnM

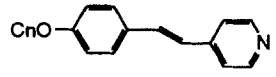

CnP

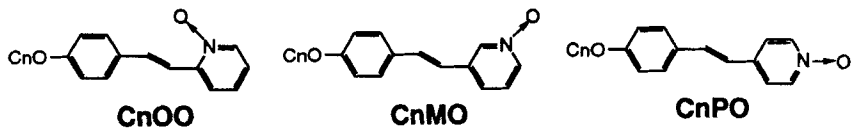

CnOO **CnMO** **CnPO**

n = 8, 12, and 16

RESULTS AND DISCUSSION

We have successfully prepared trans-stilbazoles and analogous N-oxides, i.e. 4-alkoxy-2′-stilbazoles **2** (CnO), 4-alkoxy-3′-stilbazoles **3** (CnM), 4-alkoxy-4′-stilbazoles **4** (CnP), 4-alkoxy-2′-stilbazole *N*-Oxides **5** (CnOO), 4-alkoxy-3′-stilbazole *N*-Oxides **6** (CnMO) and 4-alkoxy-4′-stilbazole *N*-Oxides **7** (CnPO). The synthetic routes of trans-stilbazoles **2–4** and their corresponding N-oxides **5–7** are shown in Scheme 1. The phosphonium salts **1** were prepared according to the literature method.[18] The synthesis was carried out in 50 mmole scale and the yield was generally over 80 % in each step. Compounds 1 were further treated with *o-*, *m-*, *p-* pyridinecarboxaldehyde to yield the desired stilbazoles **2–4**, and then stilbazoles **2–4** were treated with *m*-CPBA to produce corresponding *N*-oxides **5–7**.

The thermal transition temperatures and their corresponding enthalpies of trans-stilbazoles **2–4** and their analogous N-oxides **5–7** with different alkoxy chain lengths OCnH2n+1 (n = 8, 12 and 16) are shown in Tables I and II. In these Tables, S_1 and S_2 are temporarily assigned as S_E and S_B respectively (confirmed by XRD and polarizing optical microscopy), and S_X is the unidentified highly ordered smectic phase. Analyzing Table I and II, all N-oxides possess higher isotropization temperatures than their analogous stilbazoles, and the N atom in the ortho-position of stilbazoles and N-oxides (CnO and CnOO) all do not possess mesogenic property. Moreover, the S_A phase is more favored in N-oxide derivatives than stilbazoles, which suggests that stronger dipole moments in N-oxides may enhance arractive forces to induce the S_A phase. In general, the positional effects of N atoms on thermal properties of stilbazoles are not so prominent as N-oxides, and new mesogenic phases have formed by tuning the position of the N-oxide function in the heterocyclic ring. For instance, the isotropization temperatures of N-oxides have the following order CnPO > CnMO > CnOO at the same chain length n, but stilbazoles do not have a clear trend. This implies that stronger dipole moments and bulky side groups in N-oxides along different directions may influence the molecular planarity and packing more

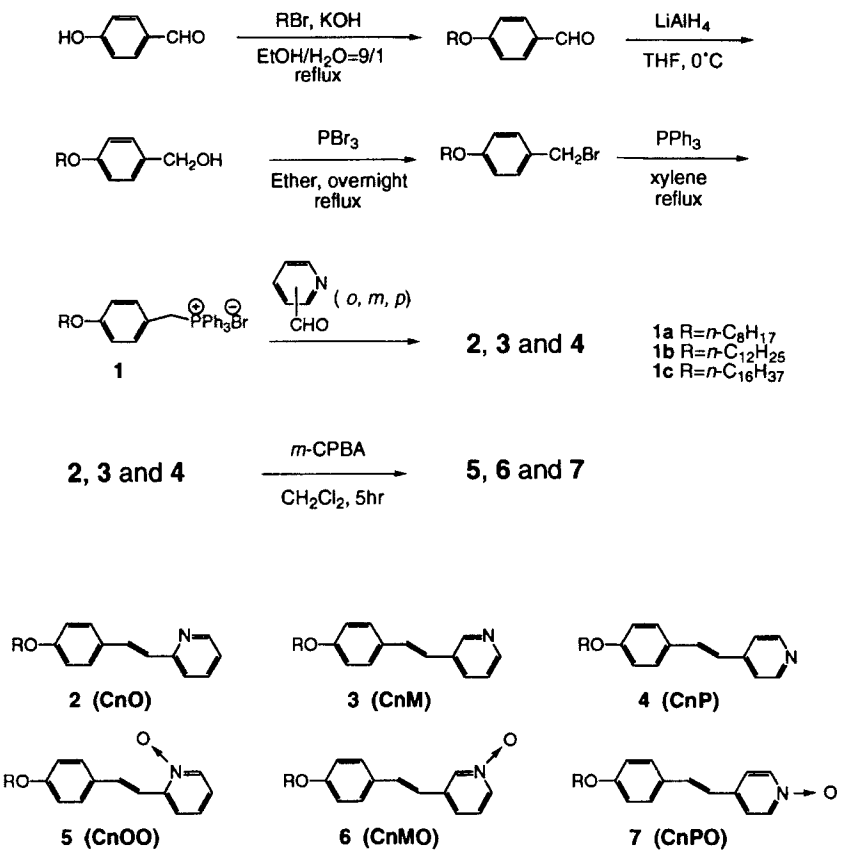

SCHEME 1 The synthetic route for compounds **2–7**

effectively than stilbazoles, and hence reduce the isotrpization temperatures sequentially. Considering stilbazoles, C8M (N atom in the meta-position and n = 8) still possesses the same phases, i.e. S_B and S_E, as C8P (the para-position). Fig. 1 shows the characteristic mosaic and lancet texture of the S_B phase[17] of C8M. However, S_B and S_E were not observed at longer chain lengths n = 12 and 16 (C12M and C16M). Comparatively, N-oxides in the meta-position (CnMO) possess extra phases, i.e. S_B and S_E, other than S_A shown in the para-position (CnPO). Fig. 2 demonstrates the mosaic texture of the S_E phase of C12MO. The smectic E phase exhibits a platelet texture which appears ghost-like images of platelets through the platelet edges as described.[19] In contrast to C16MO, C12MO and C8MO exhibit an enantiotropic S_E phase and a monotropic S_B phase respectively, which were not observed at a longer alkoxy length C16MO.

TABLE I Thermal data for trans-4-alkyloxy-2′, 3′, 4′-stilbazoles

Compound	*Transition*	*T(°C)*	$\Delta H(Jg^{-1})$
2a (C8O)	C-I	88.3	113.2
	I-S_X[a]	71.1	
	S_X-C	70.0	(112.1)[b]
2b (C12O)	C-I	85.6	116.4
	I-S_X	73.5	
	S_X-C	71.8	(114.5)
2c (C16O)	C-I	92.8	134.0
	I-S_X	82.8	
	S_X-C	82.1	(134.7)
3a (C8M)	C-S_1[a]	67.4	59.6
	S_1-S_2[a]	80.0[a]	
	S_2-I	81.8	(36.7)
	I-S_1	77.3	36.9
	S_1-C	32.9	56.3
3b (C12M)	C-I	84.0	121.1
	I-S_X	68.7	
	S_X-$S_{X'}$	66.3	
	$S_{X'}$-C	64.9	(125.6)
3c (C16M)	C-I	93.9	147.9
	I-S_X	82.0	
	S_X-C	81.4	(150.0)
4a (C8P)	C-S_E	72.9	59.1
	S_E-S_B	86.0	
	S_B-I	87.5	(38.2)
	I-S_B	82.9	
	S_B-S_E	81.4	(37.6)
	S_E-C	30.0	50.2
4b (C12P)	C-C′	84.4	
	C′-S_E	85.6	
	S_E-S_B	87.4	
	S_B-I	88.8	(127.1)
	I-S_B	78.4	33.3
	S_B-S_E	66.4	
	S_E-C	63.7	(84.5)
4c (C16P)	C-I	95.7	163.0
	I-S_X	78.7	
	S_X-C	77.8	(162.3)

a. S_X is the unidentified highly ordered smectic phase; S_1 and S_2 are assigned as S_E and S_B respectively (confirmed by XRD and POM).

b. Blank enthalpies are those overlapped phase transitions shown in the parentheses.

TABLE II Thermal data for N-oxides of trans-4-alkyloxy-2′, 3′, 4′-stilbazoles

Compound	*Transition*	*T(°C)*	$\Delta H(Jg^{-1})$
5a (C8OO)	C-I	107.7	74.8
	I-C	96.8	73.6
5b (C12OO)	C-I	109.5	73.6
	I-C	96.8	73.8
5c (C16OO)	C-I	112.6	92.2
	I-C	102.4	91.4
6a (C8MO)	$C\text{-}S_X$	78.1	2.1
	$S_X\text{-}S_2$[a]	102.3	19.8
	$S_2\text{-}I$	110.8	61.2
	$I\text{-}S_A$	107.4	7.8
	$S_A\text{-}S_X$	89.2	82.4
	$S_X\text{-}C$	53.5	0.9
6b (C12MO)	$C\text{-}S_X$	53.0	4.8
	$S_X\text{-}S_{X'}$	65.1	4.6
	$S_{X'}\text{-}S_1$[a]	89.7	19.4
	$S_1\text{-}S_A$	102.0	57. 1
	$S_A\text{-}I$	129.6	11.4
	$I\text{-}S_A$	125.9	11.5
	$S_A\text{-}S_1, S_X'$ (mixed)	82.4	58.6
	S_1, S_X' (mixed)-S_X	54.6	5.2
	$S_X\text{-}C$	39.8	3.7
6c (C16MO)	$C\text{-}S_A$	102.1	102.1
	$S_A\text{-}I$	126.9	8.3
	$I\text{-}S_A$	124.0	9.2
	$S_A\text{-}S_X$	79.5	83.5
	$S_X\text{-}C$	71.0	2.1
7a (C8PO)[b]	$C\text{-}S_A$	112.4	89. 1
	$S_A\text{-}I$	116.7	8.4
	$I\text{-}S_A$	113.4	8.5
	$S_A\text{-}C$	68.5	83.7
7b (C12PO)	$C\text{-}S_A$	108.0	96.7
	$S_A\text{-}I$	138.3	11.0
	$I\text{-}S_A$	134.9	10.7
	$S_A\text{-}C$	60.1	87.8
7c (C16PO)	$C\text{-}S_A$	100.6	100.6
	$S_A\text{-}I$	133.5	9.2
	$I\text{-}S_A$	131.0	9.1
	$S_A\text{-}C$	62.9	95.0

a. S_1 and S_2 are assigned as S_E and S_B respectively (confirmed by XRD and POM).
b. Trans-4′-hexyloxy-4-stibazole-N-oxide[16] (C6PO) : C-I (melting point) 121°C.

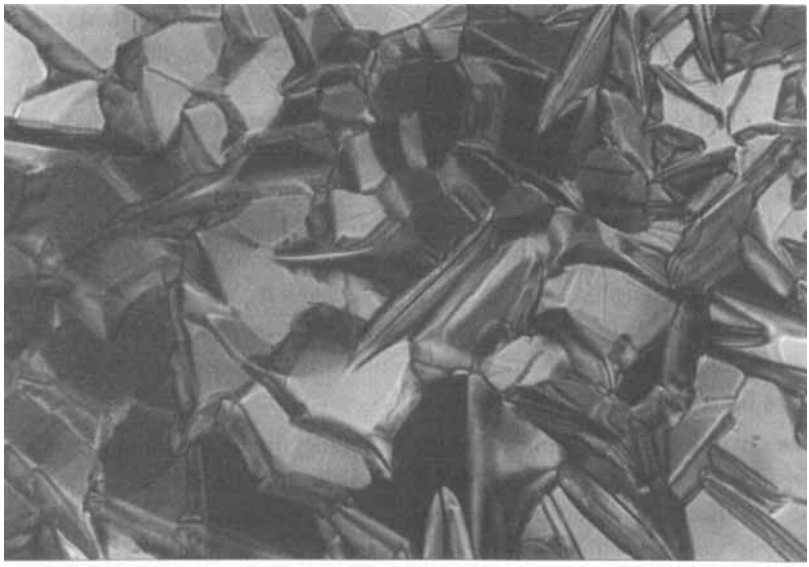

FIGURE 1 The characteristic mosaic and lancet texture of the S_B phase of C8M at 80°C (See Color Plate I at the back of this issue)

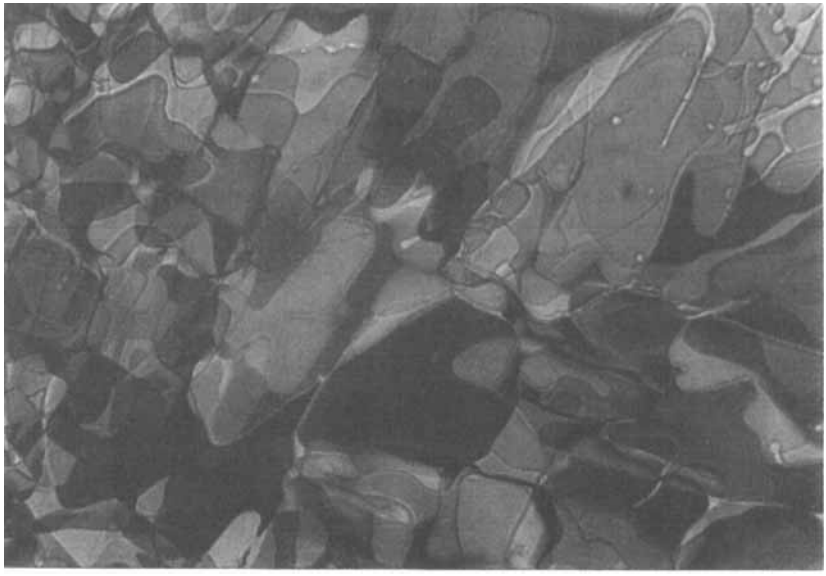

FIGURE 2 The mosaic texture of the S_E phase of C12MO at 90°C (See Color Plate II at the back of this issue)

Further, C8MO exhibits only the monotropic S_A phase, rather than the enantiotropic S_A phase in C12MO and C16MO, suggesting that the more stable enantiotropic S_A phase are not favored at the shorter alkoxy length. Regarding the para-N-oxide CnPO system, as mentioned in the literature[16] trans-4-hexyloxy-4′-stilbazole-N-oxide (C6PO) do not possess the mesogenic property and its melt point is 121°C. As $n \geq 8$, all CnPO possess the enantiotropic S_A phase and the range of the S_A phase increases as n increases. Thus, the alkoxy flexible chain length must reach a critical length $n > 6$ in order to obtain the enantiotropic S_A phase. Generally, CnPO and CnMO both exhibit broader ranges of S_A phase at longer alkoxy lengths, and CnPO exhibits a wider S_A phase than CnMO at the same n value. However, tuning the N-oxide function from the para-position (*CnPO*) to the meta-position (CnMO) can reduce the phase transition temperatures at the expense of narrower ranges of S_A phase.

The layer spacing (d) of the molecule is defined by the lowest angle of X-ray diffraction, and the d value is related to the molecular packing inside the layer. Table III shows X-ray diffraction studies of 4-dodecyloxy-2′, 3′, 4′-stilbazoles and their corresponding N-oxides. Increasing dipole moments through the charged N-oxide function is so sufficient to stabilize the layer structure S_A phase, which is proved by X-ray diffraction (XRD) to be the interdigitated bilayer structure, i.e. S_{Ad} phase. Besides, Fig. 3 shows a characteristic oily streak pattern of the S_A phase[20] of CnPO and CnMO N-oxides. This oily streak pattern of the S_A phase was also observed in another charged pyridium liquid crystals of our publication.[21] In addition, in the crystalline state a monolayer molecular packing is favored as the dipole moments of the stilbazoles and N-oxides are along the para-direction (C12P and C12PO). However, a bilayer packing is favored as the

TABLE III XRD studies of 4-dodecyloxy-2′-, 3′-, 4′- stilbazoles and their corresponding N-oxides

Compound	*Temperature(°C)*	*Phase*	*Layer spacing d(Å)*
2b (C12O)	50	C	51.3
5b (C12OO)	50	C	31.9
3b (C12M)	50	C	52.6
6b (C12MO)	50	C	43.6
	95	S_E	28.7
	120	S_A	38.7
4b (C12P)	50	C	26.0
	86	S_E	28.6
7b (C12PO)	50	C	26.6
	125	S_A	39.7

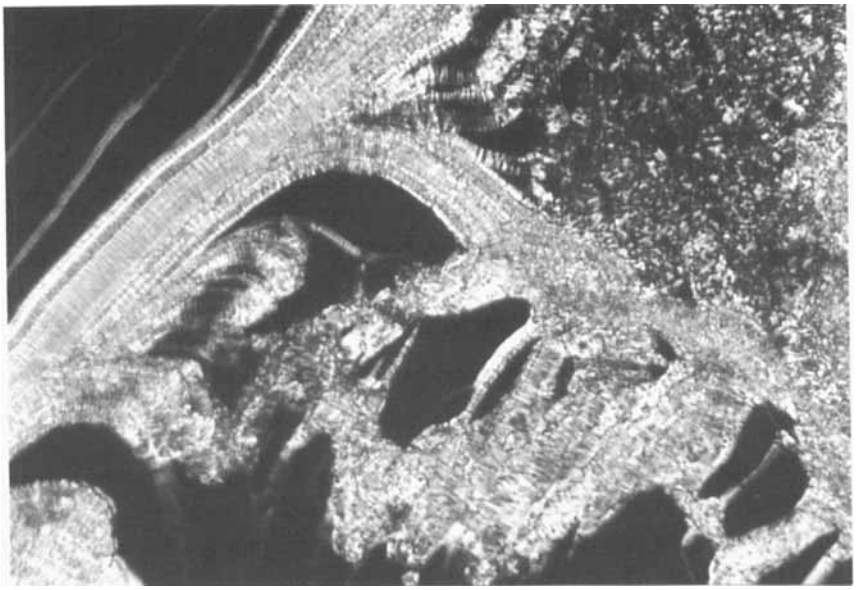

FIGURE 3 The characteristic oily streak pattern of the S_A phase of C16MO at 120°C formed on heating the crystal (at the rate of 10°C/min) (See Color Plate III at the back of this issue)

dipole moments of the stilbazoles are along the meta- and ortho- directions (C12O and C12M), and an interdigitated bilayer packing is favored as the dipole moments of the N-oxides are along the meta- and ortho- directions (C12OO and C12MO). Hence, the lateral dipole moments in the meta- and ortho- systems do facilitate the formation of the bilayer and interdigitated bilayer structures in the crystalline state. This result was confirmed by XRD and the calculation of the fully extended molecular length. The fully extended molecule (~26.4Å) and a possible molecular bilayer packing of 3b is drawn in Fig. 4. Regardless of their N-atom position, compounds **6b** and **7b** have similar layer spacings (38.7Å and 39.7Å) in the S_A phase, which is about 1.5 times of the fully extended molecular length. Based on this result, the S_A phase in compounds **6b** and **7b** can be defined as the interdigitated bilayer structure, i.e. S_{Ad} phase. This interdigitated bilayer structure may have a head-to-head arrangement with rigid cores overlapped together, which is related to the dipolar interaction between two molecules. Interestingly, the d spacing of compound **6b** varied in an unusual way as shown in Table III. Though all these molecular structures (C, S_E and S_A) are all belong to interdigitated bilayer structures, the layer thickness decreases as enter-

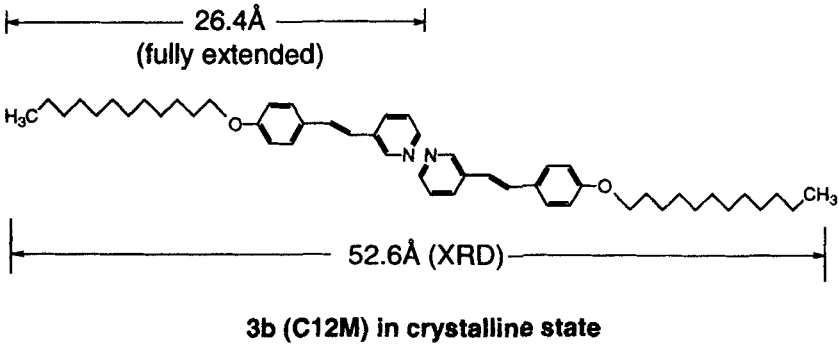

FIGURE 4 Possible molecular bilayer packing of compound **3b** in crystalline state

ing the S_E phase and increases again as entering the S_A phase during the heating cycle (reversible in the cooling cycle). Biphasic phenomenon was observed in both tranformations into and out of the S_E phase during the heating and cooling cycles. Compounds **4b** and **6b** both possess the enantiotropic S_E phase with the interdigitated bilayer packings which are approximately equal to the monolayer spacing. A possible molecular arrangement of compounds **4b** and **6b** is that the bilayer molecules in the interdigitated packing almost overlap completely in this S_E structure. Further X-ray structure analysis and the molecular modeling will be needed to explore the detailed molecular arrangement.

EXPERIMENTAL

The ^1H and ^{13}C NMR spectra were recorded on a Bruker MSL 200 spectrometer (200MHz) from a $CDCl_3$ solution with TMS as the internal standard. The elemental analyses were carried out by Perkin Elmer 2400 CHN type. The thermal transition temperatures and textures of all products were obtained from Perkin-Elmer DSC-7 and Leitz Laborlux S polarizing optical microscope (POM) equipped with a THMS-600 heating stage. The heating and cooling rates were 10°C/min for all measurements unless mentioned. Powder X-ray diffraction (XRD) patterns were obtained from a X-ray diffractometer Siemens D-5000 (40kV, 30mA) fitted with a temperature controller TTK450. Nickel-filtered CuKα radiation was used as an incident X-ray beam.*O-*, *m-* and *p-* pyridinecarboxaldehyde, alkyl bromides, lithium aluminium hydride, and phosphorus tribromide were commerciable available. Solvents were distilled before use.

Alkoxybenzyl triphenylphosphonium bromide

(a) Preparation of p-alkoxybenzaldehyde

KOH (4.2 g, 75 mmole) was dissolved in ethanol-water (100 ml; 9:1), and *p*-hydroxybenzaldehyde (6.1 g, 50 mmole) followed by 1.3 equivalents of bromoalkane was added. The resulting solution was heated under reflux for 4 hours. Water (100 ml) was added and the resulting solution was extracted with CH_2Cl_2 (50 ml × 2). The combined extracts were dried over Na_2SO_4 and evaporated at reduced pressure and purified by chromatography on silica to give the desired products in 84–98% yields.

(b) Preparation of p-alkoxybenzyl alcohol

The *p*-alkoxybenzaldehyde (50 mmole) was dissolved in THF (50–100 ml), and excess of the $LiAlH_4$ was added portion by portion. The resulting solution was stirred for 1 hour. Ice-water (100 g) was added and the resulting solution was extracted with $CHCl_3$ (200 ml). The organic solvent was dried over Na_2SO_4 and evaporated at reduced pressure and purified by chromatography on silica to give the desired products in quantitative yields.

(c) Preparation of p-alkoxybenzyl bromide

The *p*-alkoxybenzyl alcohol (50 mmole) was treated with phosphorus tribromide (25 mmole) in absolute ether (50 ml) overnight.[22] The mixture was hydrolyzed with ice water, and the layers separated. The ether layer was washed with sodium bicarbonate solution and dried over Na_2SO_4. Then, it was evaporated at reduced pressure and purified by chromatography on silica to give the desired products in 80–90% yields.

(d) Preparation of alkoxybenzyl triphenylphosphonium bromide

The *p*-alkoxybenzyl bromide (50 mmole) and 1.1 equivalents of triphenylphosphine were added to xylene (50–100 ml), and the resulting solution was heated under reflux for 2–3 hours and cooled to room temperature. Hexane (100–200 ml) was added to precipitate the solid which was then filtered and dried. The desired products was obtained in 80–90% yields.

1a: δ ($CDCl_3$) 0.88 (t, 3H, CH_3), 0.98–1.76 (m, 12H, 6xCH_2), 3.85 (t, 2H, OCH_2), 5.25 (d, 2H, J=13.68Hz, P-CH_2), 6.64 (d, 2H, J=8.50Hz, 2xAr-H), 6.99 (d, 2H, J=8.38Hz, J=8.61Hz, 2xAr-H), 7.58–7.81 (m, 15H, PPh_3-H).

1b: δ ($CDCl_3$) 0.88 (t, 3H, CH_3), 1.19–1.43 (m, 18H, 9xCH_2), 1.68–1.75 (m, 2H, CH_2), 3.84 (t, 2H, OCH_2), 5.23 (d, 2H, J=13.71Hz, P-CH_2), 6.64 (d, 2H,

J=8.48Hz, 2xAr-H), 6.98 (d, 2H, J=8.36Hz, J=8.61Hz, 2xAr-H), 7.59–7.79 (m, 15H, PPh_3-H).

1c: δ ($CDCl_3$) 0.88 (t, 3H, CH_3), 1.17–1.73 (m, 28H, 14xCH_2), 3.84 (t, 2H, OCH_2), 5.18 (d, 2H, J=13.65Hz, P-CH_2), 6.63 (d, 2H, J=8.34Hz, 2xAr-H), 6.97 (d, 2H, J=8.41Hz, J=8.65Hz, 2xAr-H), 7.58–7.82 (m, 15H, PPh_3-H).

Trans-4-alkyloxy-2′-, 3′-, 4′-stilbazoles

Pyridinecarboxaldehyde (0.21g, 2 mmole) and 1.2 equivalents of the dried alkoxybenzyl triphenylphosphonium bromide were disolved in ethanol (30 ml) and 2.4 mmole of ETOLi (0.2 M, 12 ml in ethanol) was then added. The resulting solution was stirred for 30 minutes. Water (50 ml) was added and the resulting solution was extracted with CH_2Cl_2 (50 ml x2).

The combined extracts were dried over Na_2SO_4 and evaporated at reduced pressure and purified by chromatography on silica to give the desired stilbazoles in 30–50% yields.

2a: ^{1}H NMR δ ($CDCl_3$) 0.89 (t, 3H, CH_3), 1.26–1.45 (m, 10H, 5xCH_2), 1.75–1.81 (m, 2H, CH_2), 3.96 (t, 2H, OCH_2), 6.89 (d, 2H, J=8.66Hz, 2xAr-H), 7.34 (d, 1H, J=7.82Hz, Ar-H), 7.50 (d, 2H, J=8.64Hz, 2xAr-H), 8.57 (d, 1H, J=2.99Hz, Ar-H), 7.01–7.11, 7.56–7.65 (2m, 4H, 2xAr-H+2xCH=). ^{13}C NMR δ ($CDCl_3$)14.05, 22.62, 26.02, 29.21, 29.32, 31.78, 68.08, 114.74, 121.56, 121.68, 125.47, 128.42, 129.18, 132.57, 136.51, 149.39, 155.97, 159.54. Elemental analysis: calculated: C=81.51, H=8.79, N=4.53; experimental: C=81.67, H=9.09, N=4.35.

2b: ^{1}H NMR δ ($CDCl_3$) 0.88 (t, 3H, CH_3), 1.27–1.46 (m, 18H, 9xCH_2), 1.76–1.83 (m, 2H, CH_2), 3.98 (t, 2H, OCH_2), 6.89 (d, 2H, J=8.67Hz, 2xAr-H), 7.37 (d, 1H, J=7.80Hz, Ar-H), 7.51 (d, 2H, J=8.53Hz, 2xAr-H), 8.59 (s, 1H, Ar-H), 7.02–7.14, 7.57–7.65 (2m, 4H, 2xAr-H+2xCH=). ^{13}C NMR δ ($CDCl_3$)14.08, 22.67, 26.03, 29.37, 29.62, 31.91, 68.14, 114.29, 114.81, 121.68, 124.87, 128.57, 129.06, 130.29, 133.22, 137.00, 148.89, 159.71. Elemental analysis: calculated: C=82.14, H=9.65, N=3.83; experimental: C=81.96, H=9.81, N=3.78.

2c: ^{1}H NMR δ ($CDCl_3$) 0.88 (t, 3H, CH_3), 1.26–1.46 (m, 26H, 13xCH_2), 1.74–1.83 (m, 2H, CH_2), 3.98 (t, 2H, OCH_2), 6.89 (d, 2H, J=8.65Hz, 2xAr-H), 7.35 (d, 1H, J=7.94,Hz Ar-H), 7.50 (d, 2H, J=8.69Hz, 2xAr-H), 8.58 (d, 1H, J=3.98Hz, Ar-H), 7.01–7.13, 7.55–7.66 (2m, 4H, 2xAr-H+2xCH=). ^{13}C NMR δ ($CDCl_3$) 14.09, 22.68, 26.04, 29.26, 29.38, 29.68, 31.92, 68.12, 114.77, 121.60, 121.70, 125.50, 128.44, 129.20, 132.59, 136.54, 149.43, 159.55. Elemental analysis: calculated: C=82.61, H=10.28, N=3.32; experimental: C=82.51, H=10.59, N=3.28.

3a: ^{1}H NMR δ ($CDCl_3$) 0.89 (t, 3H, CH_3), 1.23–1.49 (m, 10H, 5xCH_2), 1.74–1.84 (m, 2H, CH_2),3.98 (t, 2H, OCH_2), 6.89 (d, 2H, J=8.43Hz, 2xAr-H), 6.91 (d,

1H, J=10.27Hz, CH=), 7.11 (d. 1H, J=16.32Hz, CH=), 7.24–7.29 (m, 1H, Ar-H), 7.44 (d, 2H, J=8.74Hz, 2xAr-H), 7.80 (d, 1H, J=6.33Hz, Ar-H), 8.44+8.69 (2s, 2H, 2xAr-H). ^{13}C NMR δ ($CDCl_3$) 14.04, 22.62, 26.01, 29.21, 29.31, 31.54, 31.77, 68.10, 114.79, 122.37, 123.51, 127.90, 129.17, 130.57, 132.51, 133.49, 147.78, 148.02, 159.38. Elemental analysis: calculated: C=81.51, H=8.79, N=4.53; experimental: C=81.44, H=8.67, N=4.47.

3b: ^{1}H NMR δ ($CDCl_3$) d 0.88 (t, 3H, CH_3), 1.27–1.46 (m, 18H, 9xCH_2), 1.75–1.83 (m, 2H, CH_2),3.98 (t, 2H, OCH_2), 6.90 (d, 2H, J=8.55Hz, 2xAr-H), 6.92 (d, 1H, J=8.81Hz, CH=), 7.11 (d, 1H, J=16.41Hz, CH=), 7.26–7.29 (m, 1H, Ar-H), 7.45 (d, 2H, J=8.65Hz, 2xAr-H), 7.77 (d, 1H, J=7.93Hz, Ar-H), 8.46+8.59 (2s, 2H, 2xAr-H). ^{13}C NMR δ ($CDCl_3$)14.09, 22.67, 26.03, 29.26, 29.35, 29.61, 31.57, 31.91, 68.14, 114.82, 122.34, 123.65, 127.95, 129.18, 130.71, 132.65, 147.59, 147.86, 159.44. Elemental analysis: calculated: C=82.14, H=9.65, N=3.83; experimental: C=82.32, H=9.81, N=3.49.

3c: ^{1}H NMR δ ($CDCl_3$) 0.88 (t, 3H, CH_3), 1.26–1.48 (m, 26H, 13xCH_2), 1.76–1.81 (m, 2H, CH_2),3.97 (t, 2H, OCH_2), 6.89 (d, 2H, J=8.43Hz, 2xAr-H), 6.92 (d, 1H, J=17.47Hz, CH=), 7.12 (d, 1H, J=16.42Hz, CH=), 7.26–7.28 (m, 1H,Ar-H), 7.44 (d, 2H, J=8.67Hz, 2xAr-H), 7.79 (d, 1H, J=7.89Hz, Ar-H), 8.46+8.70 (2s, 2H, 2xAr-H). ^{13}C NMR δ ($CDCl_3$)14.06, 22.65, 26.01, 29.23, 29.35, 29.57, 29.65, 31.90, 68.11, 114.79, 122.43, 123.50, 127.90, 129.20, 130.53, 132.44, 133.45, 147.88, 148.11, 159.38. Elemental analysis: calculated: C=82.61, H=10.28, N=3.32; experimental: C=82.61, H=10.55, N=3.06.

4a: ^{1}H NMR δ ($CDCl_3$) 0.89 (t, 3H, CH_3), 1.26–1.48 (m, 10H, 5xCH_2), 1.74–1.81 (m, 2H, CH_2), 3.98 (t, 2H, OCH_2), 6.86 (d, 1H, J=16.22Hz, CH=), 6.92 (d, 2H, J=8.72Hz, 2xAr-H), 7.26 (d, 1H, J=16.27Hz, CH=), 7.34 (d, 2H, J=3.93Hz, 2xAr-H), 7.46 (d, 2H, J=8.72Hz, 2xAr-H), 8.55 (s, 2H, 2xAr-H). ^{13}C NMR δ ($CDCl_3$) 14.04, 22.62, 26.00, 29.20, 29.31, 29.66, 31.77, 68.13, 114.84, 120.72, 123.40, 128.39, 128.60, 133.11, 145.40, 149.64, 159.86. Elemental analysis: calculated: C=81.51., H=8.79, N=4.53; experimental: C=81.92, H=9.23, N=4.40.

4b: ^{1}H NMR δ ($CDCl_3$) 0.88 (t, 3H, CH_3), 1.27–1.48 (m, 18H, 9xCH_2), 1.76–1.81 (m, 2H, CH_2), 3.98 (t, 2H, OCH_2), 6.86 (d, 1H, J=16.22Hz, CH=), 6.90 (d, 2H, J=8.69Hz, 2xAr-H), 7.27 (d, 1H, J=16.27Hz, CH=), 7.35 (s, 2H, 2xAr-H), 7.46 (d, 2H, J=8.66Hz, 2xAr-H), 8.58 (s, 2H, 2xAr-H). ^{13}C NMR δ ($CDCl_3$)14.08, 22.67, 26.01, 29.22, 29.34, 29.61, 31.90, 68.15, 114.87, 120.87, 123.40, 128.42, 128.61, 133.21, 145.49, 149.55, 159.90. Elemental analysis: calculated: C=82.14, H=9.65, N=3.83; experimental: C=81.97, H=9.82, N=3.76.

4c: ^{1}H NMR δ ($CDCl_3$) 0.88 (t, 3H, CH_3), 1.19–1,81 (m, 28H, 14xCH_2), 3.98 (t, 2H, OCH_2), 6.86 (d, 1H, J=16.08Hz, CH=), 6.90 (d, 2H, J=8.52Hz, 2xAr-H), 7.27 (d, 1H, J=16.32Hz, CH=), 7.33 (d, 2H, J=5.55Hz, 2xAr-H), 7.46 (d, 2H, J=8.61Hz, 2xAr-H), 8.54 (s, 2H, 2xAr-H). ^{13}C NMR δ ($CDCl_3$) 14.08, 22.66,

26.01, 29.21, 29.35, 29.66, 31.91, 68.14, 114.85, 120.64, 123.47, 128.37, 133.00, 145.27, 149.82, 159.85. Elemental analysis: calculated: C=82.61, H=10.28, N=3.32; experimental: C=82.71, H=10.30, N=2.98.

Trans-4-alkyloxy-2′-, 3′-, 4′-stilbazole-N-oxides

m-CPBA (3.44 g, 2 mmole) was added to the stilbazole (2 mmole) in dichloromethane (30 mL) and the resulting mixture was stirred for 5 hours at room temperature. Solvent was removed at reduced pressure and the residue was recrystallized from hexane to give the desired *N*-oxides **5**, **6** and **7** in 80–90 % yields.

5a: ^{1}H NMR δ ($CDCl_3$) 0.89 (t, 3H, CH_3), 1.30–1.49 (m, 10H, 5 × CH_2), 1.79 (m, 2H, CH_2), 3.98 (t, 2H, OCH2), 6.90 (d, 2H, J=8.71Hz, 2 × Ar-H), 7.04–7.11 (m, 1H, Ar-H), 7.21 (t, 1H, Ar-H), 7.37 (d, 1H, J=16.71Hz, CH=), 7.54 (d, 2H, J=8.72Hz, 2 × Ar-H), 7.58–7.63 (m, 1H, Ar-H), 7.70 (d, 1H, J=16.69, CH=), 8.23 (d, 1H, J=6.22, Ar-H). ^{13}C NMR δ ($CDCl_3$) 14.02, 22.57, 25.96, 29.15, 29.27, 31.74, 68.07, 114.74, 116.14, 122.40, 122.93, 125.35, 128.65, 128.89, 135.24, 139.80, 148.20, 160.08. Elemental analysis: calculated: C=77.50, H=8.36, N=4.30; experimental: C=77.49, H=8.36, N=4.27.

5b: ^{1}H NMR δ ($CDCl_3$) 0.88 (t, 3H, CH_3), 1.27–1.44 (m, 18H, 9 × CH_2), 1.72–1.86 (m, 2H, CH_2), 3.98 (t, 2H, OCH_2), 6.90 (d, 2H, J=8.69Hz, 2 × Aρ-H), 7.03–7.11 (m, 1H, Ar-H), 7.21 (t, 1H, Ar-H), 7.37 (d, 1H, J=16.68Hz, CH=), 7.54 (d, 2H, J=8.72Hz, 2 × Ar-H), 7.58–7.63 (m, 1H, Ar-H), 7.70 (d, 1H, J=16.68, CH=), 8.23 (d, 1H, J=6.44, Ar-H). ^{13}C NMR δ ($CDCl_3$) 14.05, 22.61, 25.96, 29.15, 29.28, 29.32, 29.51, 29.57, 29.59, 31.84, 68.07, 114.75, 116.13, 122.41, 122.93, 125.37, 128.65, 128.90, 135.26, 139.82, 148.22, 160.08. Elemental analysis: calculated: C=78.70, H=9.25, N=3.67; experimental: C=78.67, H=9.27, N=3.74.

5c: ^{1}H NMR δ ($CDCl_3$) 0.88 (t, 3H, CH_3), 1.18–1.45 (m, 26H, 13 × CH_2), 1.79 (m, 2H, CH_2), 3.98 (t, 2H, OCH_2), 6.90 (d, 2H, J=8.21Hz, 2 × Ar-H), 7.04–7.13 (m, 1H, Ar-H), 7.23 (t, 1H, Ar-H), 7.38 (d, 1H, J=16.68Hz, CH=), 7.55 (d, 2H, J=8.77Hz, 2 × Ar-H), 7.60–7.65 (m, 1H, Ar-H), 7.71 (d, 1H, J=16.68, CH=), 8.25 (d, 1H, J=6.02, Ar-H). ^{13}C NMR δ ($CDCl_3$) 14.08, 22.64, 25.99, 29.18, 29.32, 29.35, 29.54, 29.65, 31.89, 68.09, 114.76, 116.10, 122.42, 122.97, 125.51, 128.64, 128.93, 135.33, 139.85, 148.26, 160.11. Elemental analysis: calculated: C=79.59, H=9.90, N=3.20; experimental: C=79.54, H=9.88, N=3.32.

6a: ^{1}H NMR δ ($CDCl_3$) 0.89 (t, 3H, CH_3), 1.30–1.49 (m, 10H, 5 × CH_2), 1.79 (quint, 2H, CH_2), 3.98 (t, 2H, OCH_2), 6.75 (d, 1H, J=16.30Hz, CH=), 6.90 (d, 2H, J=8.70Hz, 2 × Ar-H), 7.11(d, 1H, J=16.32, CH=), 7.20–7.28 (m, 1H, Ar-H), 7.39 (d, 1H, J=9.66, Ar-H), 7.44 (d, 2H, J=8.76Hz, 2 × Ar-H), 8.07 (d, 1H, J=6.05, Ar-H), 8.32 (s, 1H, Ar-H). ^{13}C NMR δ ($CDCl_3$) 14.00, 22.56, 25.93,

29.12, 29.25, 31.71, 68.08, 114.80, 119.64, 123.27, 125.59, 128.09, 128.30, 133.19, 136.77, 136.92, 137.24, 159.92. Elemental analysis: calculated: C=77.50, H=8.36, N=4.30; experimental: C=77.05, H=8.38, N=4.29.

6b: ^{1}H NMR δ ($CDCl_3$) 0.88 (t, 3H, CH_3), 1.27–1.49 (m, 18H, 9 × CH_2), 1.73–1.86 (m, 2H, CH_2), 3.98 (t, 2H, OCH_2), 6.75 (d, 1H, J=16.40Hz, CH=), 6.91 (d, 2H, J=8.70Hz, 2 × Ar-H), 7.12(d, 1H, J=16.30, CH=), 7.20–7.27 (m, 1H, Ar-H), 7.39 (d, 1H, J=9.68, Ar-H), 7.44 (d, 2H, J=8.80Hz, 2 × Ar-H), 8.08 (d, 1H, J=6.13, Ar-H), 8.33 (s, 1H, Ar-H). ^{13}C NMR δ ($CDCl_3$) 14.01, 22.65, 25.98, 29.16, 29.32, 31.71, 68.08, 114.85, 119.69, 123.35, 125.63, 128.09, 128.35, 133.24, 136.82, 136.95, 137.39, 159.97. Elemental analysis: calculated: C=78.70, H=9.25, N=3.67; experimental: C=78.22, H=9.22, N=3.68.

6c: ^{1}H NMR δ ($CDCl_3$) 0.88 (t, 3H, CH_3), 1.25–1.45 (m, 26H, 13 × CH_2), 1.73–1.83 (m, 2H, CH_2), 3.98 (t, 2H, OCH_2), 6.75 (d, 1H, J=16.34Hz, CH=), 6.91 (d, 2H, J=8.74Hz, 2 × Ar-H), 7.12(d, 1H, J=16.34, CH=), 7.21–7.27 (m, 1H, Ar-H), 7.40 (d, 1H, J=9.46, Ar-H), 7.44 (d, 2H, J=8.78Hz, 2 × Ar-H), 8.07 (d, 1H, J=5.26, Ar-H), 8.33 (s, 1H, Ar-H). ^{13}C NMR δ ($CDCl_3$) 14.08, 22.66, 25.97, 29.16, 29.34, 29.52, 29.55, 29.61, 29.65, 31.89, 68.11, 114.84, 119.67, 123.30, 125.63, 128.12, 128.35, 133.22, 136.84, 137.27, 137.39, 159.95. Elemental analysis: calculated: C=79.59, H=9.90, N=3.20; experimental: C=79.70, H=10.08, N=3.16.

7a: ^{1}H NMR δ ($CDCl_3$) 0.89 (t, 3H, CH_3), 1.26–1.82 (m, 12H, 6xCH_2), 3.98 (t, 2H, OCH_2), 6.83 (d, 1H, J=16.58Hz, CH=), 6.91 (d, 2H, J=8.60Hz, 2 × Ar-H), 7.11 (d, 1H, J=15.47, CH=), 7.35 (s, 2H, 2 × Ar-H), 7.44 (d, 2H, J=8.64Hz, 2 × Ar-H), 8.14 (d, 2H, J=6.36Hz, 2 × Ar-H) ^{13}C NMR δ ($CDCl_3$) 14.08, 22.67, 26.00, 29.18, 29.66, 31.90, 68.20, 114.98, 120.98, 122.64, 128.04, 128.66, 129.57, 130.05, 132.81, 134.32, 137.34, 160.31. Elemental analysis: calculated: C=77.50, H=8.36, N=4.30; experimental: C=77.24, H=8.39, N=4.30.

7b: ^{1}H NMR δ ($CDCl_3$) 0.88 (t, 3H, CH_3), 1.26–1.49 (m, 18H, 9 × CH_2), 1.76–1.82 (m, 2H, CH_2), 3.98 (t, 2H, OCH_2), 6.80 (d, 1H, J=16.60Hz, CH=), 6.91 (d, 2H, J=8.58Hz, 2 × Ar-H), 7.16 (d, 1H, J=16.36Hz, CH=), 7.35 (d, 2H, J=11.36Hz,2 × Ar-H), 7.44 (d, 2H, J=8.64Hz, 2 × Ar-H), 8.14 (d, 2H, J=6.92Hz, 2 × Ar-H). ^{13}C NMR δ ($CDCl_3$) 14.09, 22.68, 29.18, 29.35, 29.64, 31.91, 68.20, 114.98, 120.98, 122.63, 128.06, 128.60, 129.58, 130.06, 132.88, 134.48, 137.22, 160.12. Elemental analysis: calculated: C=78.70, H=9.25, N=3.67; experimental: C=78.40, H=9.19, N=3.77.

7c: ^{1}H NMR δ ($CDCl_3$) 0.88 (t, 3H, CH_3), 1.25–1.45 (m, 26H, 13 × CH_2), 1.73–1.83 (m, 2H, CH_2), 3.98 (t, 2H, OCH_2), 6.85 (d, 1H, J=16.74Hz, CH=), 6.91 (d, 2H, J=8.87Hz, 2 × Ar-H), 7.19 (d, 1H, J=16.34, CH=), 7.40 (d, 1H, J=9.46, Ar-H), 7.47 (d, 2H, J=8.11Hz, 2 × Ar-H), 8.16 (d, 2H, J=6.98Hz, 2 × Ar-H). ^{13}C NMR δ ($CDCl_3$) 14.08, 22.67, 26.00, 29.18, 29.66, 31.90, 68.20,

114.98, 120.98, 122.64, 128.04, 128.66, 129.57, 130.05, 132.81, 134.32, 137.34, 160.31. Elemental analysis: calculated: C=79.59, H=9.90, N=3.20; experimental: C=79.58, H=9.78, N=3.08.

CONCLUSION

Though compounds **2–7** do not have remarkable changes in the chemical structure, pronounced effects on the mesogenic behavior occur owing to the strengths and directions of the dipole monents originated from the different nitrogen positions in the heterocyclic rigid cores. Importantly, increasing dipole moments by oxidation of the stilbazoles to the analogous N-oxides induces the S_A phase and also enhances the interdigitated bilayer packing. Moreover, the positonal effects of the N-oxides on mesogenic properties are more distinct than those of analogous stilbazoles, and new mesogenic phases have formed by tuning the position of the N-oxide function in the heterocycles. In addition to the generation of new mesogenic phases, changing the direction of the dipole moments in N-oxides from the para-direction to the meta-direction may also reduce the phase transition temperatures at the expense of the ranges of the mesogenic phases. However, mesogenic phases are not favored in both 2′-stilbazoles and their corresponding N-oxides. This phenomenon may be due that π electron polarizabilities were reduced by the molecular twist originated from dipoles. Overall, modifying molecules with different dipolar strengths and directions may have diversified shapes and sizes of the molecular architecture and, we believe, it will result in the interesting and different liquid crystalline behavior.

Acknowledgements

This work was funded by the Institute of Chemistry, Academia Sinica and the National Science Council of the Republic of China through Grant No. NSC 85–2113-M-001–009.

References

1. a) L. -L. Lai, C. H. Wang, W. P. Hsieh and H. C. Lin, *Mol. Cryst. Liq. Cryst.*, **287**, 177 (1996).
   b) H. C. Lin, L. -L. Lai, W. P. Hsieh and W. Y. Huang, *Liq. Crystals*, **22**, 661 (1997).
2. A. I. Pavluchenko, N. I. Smirnova, V. F. Petrov, M. F. Grebyonkin and V. V. Titov, *Mol. Cryst. Liq. Cryst.*, **209**, 155 (1991).
3. a) S. M. Kelly and J. Funfschilling, *Liq. Crystals*, **19**, 519 (1995).
   b) S. M. Kelly and J. Funfschilling, *Liq. Crystals*, **20**, 77 (1996).
4. C. Zuniga, J. Belmar, M. Parra, A. Ramirez, J. Decap, B. Ros and J. L. Serrano, *Liq. Crystals*, **20**, 253 (1996).
5. D. Coates, *Liquid Crystals – Application and uses 1*, edited by B. Birendra (World Scientific), Chapter 3 (1990).
6. H. Schubert and H. Zaschke, *J. Prakt. Chem.*, **312**, 494 (1970).

7. M. P. Burrow, G.W. Gray, D. Lacey and K. J. Toyne, *Liq. Crystals*, **3**, 1643 (1988).
8. J. W. Goodby, E. Chin, T. M. Leslie, J. M. Geary and J. S. Patel, *J. Am. Chem. Soc.*, **108**, 4729 (1986).
9. D. Coates, *Liquid Crystals*, **2**, 423 (1987).
10. C. Loubser and J. W. Goodby, *J. Mater. Chem.*, **5**, 1107 (1995).
11. L. K. M. Chan, G. W. Gray and D. Lacey, *Mol. Cryst. Liq. Cryst.*, **123**, 185 (1985).
12. S. M. Kelly, J. Funfschilling, and F. Leenhouts, *Liquid Crystals*, **10**, 243 (1991).
13. a) T. Kato, H. Kihara, U. Kumar, T. Uryu and J. M. J. Fréchet, *Angew. Chem. Int. Ed. Engl.*, **33**, 1644 (1994).
    b) T. Kato, H. Kihara, T. Uryu, A. Fujishima and J. M. J. Fréchet, *Macromolecules*, **25**, 6836 (1992).
    c) T. Kato, T. Uryu, F. Kaneuchi, C. Jin and J. M. J. Fréchet, *Liq. Crystals*, **25**, 6836 (1993).
14. a) D. J. Byron, D. Lacey and R. C. Wilson, *Mol. Cryst. Liq. Cryst.*, **75**, 225 (1981).
    b) D. J. Byron, D. Lacey and R. C. Wilson, *Mol. Cryst. Liq. Cryst.*, **76**, 253 (1981).
15. D. Guillon, A. Skoulios, D. J. Byron and R. C. Wilson, *Mol. Cryst. Liq. Cryst.*, **116**, 123 (1984).
16. U. Kumar and J. M. J. Fréchet, *Adv. Mater.*, **4**, 665 (1992).
17. D. W. Bruce, D. A. Dunmur, E. Lalinde, P. M. Maitlis and P. Styring, *Liq. Crystals*, **3**, 385 (1988).
18. B. S. Furniss, A. J. Hannaford, P. W. G. Smith and A. R. Tatchell, *Vogel's Textbook of Practical Organic Chemistry*, (Longman Scientific and Technical), Chapters 5 and 6 (1989), and references cited theirin.
19. G. W. Gray and J. W. G. Goodby, *Smectic Liquid Crystals*, Leonard Hill, (1984).
20. Y. Kosaka, T. Kato and T. Uryu, *Liq. Crystals*, **18**, 693 (1995).
21. H.C. Lin, W. L. Chia, Y. K. Shiaw, C. N. Chen, IUPAC Polymer Symposium Preprints, 449 (1994).
22. W. Q. Beard, Jr., D. N. Van eenam and C. R. Hauser, *J. Org. Chem.*, **26**, 2310 (1961).